Available online at www.sciencedirect.com
SCIENCE DIRECT®
Journal of Sound and Vibration 286 (2005) 167–186
JOURNAL OF SOUND AND VIBRATION
www.elsevier.com/locate/jsvi

Free flexural vibration behavior of bimodular material angle-ply laminated composite plates

B.P. Patel*, S.S. Gupta, R. Sarda[1]

Mechanical Engineering Faculty, Institute of Armament Technology, Girinagar, Pune-411 025, India

Received 2 April 2004; received in revised form 13 July 2004; accepted 1 October 2004
Available online 20 December 2004

Abstract

In this paper, the free flexural vibration behavior of bimodular laminated angle-ply composite plates is studied. The formulation is based on the theory that accounts for the transverse shear and transverse normal deformations, and incorporates higher order through the thickness approximations of the in-plane and transverse displacements. The governing equations obtained using Lagrange's equations of motion are solved through the finite element approach. A detailed parametric study is carried out to study the influences of plate geometry, lay-up, ply-angle and material properties on the free flexural vibration response and frequencies, neutral surface locations and mode shapes of bimodulus angle-ply composite laminated plates.

1. Introduction

Certain fiber-reinforced composite materials, e.g. aramid–rubber, polyester–rubber, carbon–carbon composites, soft biological tissues, etc., exhibit different elastic behavior in tension and compression. Their actual stress–strain relationship is nonlinear, which is often approximated by two straight lines with a slope discontinuity at the origin. Such bilinear material

*Corresponding author. Tel.: +91 020 24389744; fax: +91 020 24389509.
E-mail address: badripatel@hotmail.com (B.P. Patel).
[1]Post-graduate student.

0022-460X/$ - see front matter © 2004 Elsevier Ltd. All rights reserved.
doi:10.1016/j.jsv.2004.10.004

models are termed as bimodulus material models. The fiber-governed symmetric compliance bimodulus material model, consistent with the experimental data for several materials proposed by Bert [1], is commonly employed for the analysis of bimodular structures. Some of the other examples of bimodulus materials are unidirectional glass fibers in an epoxy matrix having compression moduli about 0.8 times the tension moduli, boron/epoxy with compression moduli about 1.2 times the tension moduli, graphite/epoxy laminates having tension moduli higher than compression moduli (about 40%), carbon/carbon composites having tension moduli varying from two to five times greater than the compression moduli [2]. The analysis of bimodular laminates is more complicated than that of ordinary laminates since the elastic moduli depend on the sign of the fiber direction strains, which are unknown a priori.

The static bending analyses of laminates of bimodulus materials have attracted the attention of many researchers [3–14]. These studies are based on either the classical plate theory or first-order shear deformation theory. The exact solution of composite laminates [15,16] indicates that the first-order theories do not adequately model the behavior of thick highly orthotropic composite laminates in addition to the requirement of an arbitrary shear correction factor. The application of higher-order theories for the study of thick bimodular multi-layered laminates seems to be scarce in the literature [17–19]. All these works [17–19] are concerned with the cross-ply laminates and provide results for displacements and neutral surface locations. Further, the stress analysis of such plates has received very limited attention in the literature [20,21]. The hybrid stress approach is employed considering cross-ply bimodular laminates in the work of Tseng and Jiang [20], whereas failure and damage analysis is carried out using layerwise theory in Ref. [21].

The dynamic analysis of bimodular laminates has received the attention of few researchers [22–29]. Doong and Chen [22] and Chen and Juang [23] have studied the axisymmetric free vibration behavior of single-layer orthotropic bimodular circular/annular plates using first-order shear deformation theory, whereas the asymmetric free vibration and dynamic stability behaviors of similar structures are analyzed in the work of Chen and Chen [24]. The transient response analysis of bimodular beams is studied in Ref. [25] using the transfer matrix method and that of the single-layer orthotropic/two-layered cross-ply bimodular plates is studied by Reddy [26], employing analytical/finite element approaches based on first-order shear deformation theory. The free flexural vibration analysis of single-layer orthotropic/two-layered cross-ply bimodular rectangular plates [27,28] and shell panels [29] has been carried out using first-order shear deformation theory using analytical/finite element methods. To the authors' knowledge, the work on the free flexural vibration characteristics of angle-ply bimodular laminates is not yet available in the literature.

Here, a C^0 eight-noded quadrilateral serendipity field consistent plate element developed based on higher order theory with 11 degrees of freedom per node is used for the free flexural vibration analysis of bimodular angle-ply laminated composite plates. The formulation is general in the sense that it is applicable for the analysis of plates with arbitrary lamination scheme, boundary conditions, thick and thin structures. A detailed parametric study is carried out to study the influences of plate geometry, lay-up, ply-angle and the material properties on the free flexural vibration frequencies, neutral surface locations and mode shapes of bimodulus angle-ply composite laminates.

2. Formulation

A composite plate with arbitrary lamination is considered with the coordinates x, y along the in-plane directions and z along the thickness direction. Based on Taylor's series expansion method for deducing the two-dimensional formulation of a three-dimensional elasticity problem, the in-plane displacements u and v, and the transverse displacement w are assumed as [18]

$$\begin{aligned} u(x,y,z) &= u_0(x,y) + z\theta_x(x,y) + z^2\beta_x(x,y) + z^3\phi_x(x,y),\\ v(x,y,z) &= v_0(x,y) + z\theta_y(x,y) + z^2\beta_y(x,y) + z^3\phi_y(x,y),\\ w(x,y,z) &= w_0(x,y) + zw_1(x,y) + z^2\Gamma(x,y). \end{aligned} \tag{1}$$

Here, u_0, v_0, w_0 are the displacements of a generic point on the reference surface; θ_x, θ_y are the rotations of the normal to the reference surface about the y and x axes, respectively; w_1, β_x, β_y, Γ, ϕ_x, ϕ_y are the higher-order terms in the Taylor's series expansions, defined at the reference surface.

The strains in terms of mid-plane deformation, rotations of normal, and higher-order terms associated with displacements are given by

$$\{\varepsilon\} = \begin{Bmatrix} \varepsilon_{\mathrm{bm}} \\ \varepsilon_s \end{Bmatrix}. \tag{2}$$

The vector $\{\varepsilon_{\mathrm{bm}}\}$ includes the bending and membrane terms of the strain components and vector $\{\varepsilon_s\}$ contains the transverse shear strain terms. These strain vectors can be defined as

$$\begin{Bmatrix} \varepsilon_{\mathrm{bm}} \\ \varepsilon_s \end{Bmatrix} = \begin{Bmatrix} \varepsilon_{xx} \\ \varepsilon_{yy} \\ \varepsilon_{zz} \\ \varepsilon_{xy} \\ \gamma_{xz} \\ \gamma_{yz} \end{Bmatrix} = \begin{Bmatrix} u_{,x} \\ v_{,y} \\ w_{,z} \\ u_{,y} + v_{,x} \\ u_{,z} + w_{,x} \\ v_{,z} + w_{,y} \end{Bmatrix} = [\bar{Z}]\{\, \varepsilon_0 \quad \varepsilon_1 \quad \varepsilon_2 \quad \varepsilon_3 \quad \gamma_0 \quad \gamma_1 \quad \gamma_2 \,\}^{\mathrm{T}}, \tag{3a}$$

where

$$[\bar{Z}] = \begin{bmatrix} [I_1] & z[I_1] & z^2[I_1] & z^3[I_1] & [O] & [O] & [O] \\ [O]^{\mathrm{T}} & [O]^{\mathrm{T}} & [O]^{\mathrm{T}} & [O]^{\mathrm{T}} & [I_2] & z[I_2] & z^2[I_2] \end{bmatrix}. \tag{3b}$$

$[I_1]$ and $[I_2]$ are identity matrices of sizes 4×4 and 2×2, respectively, and $[O]$ is a null matrix of size 4×2.

$$\{\varepsilon_0\} = \begin{Bmatrix} u_{0,x} \\ v_{0,y} \\ w_1 \\ u_{0,y} + v_{0,x} \end{Bmatrix}, \quad \{\varepsilon_1\} = \begin{Bmatrix} \theta_{x,x} \\ \theta_{y,y} \\ 2\Gamma \\ \theta_{x,y} + \theta_{y,x} \end{Bmatrix},$$

$$\{\varepsilon_2\} = \begin{Bmatrix} \beta_{x,x} \\ \beta_{y,y} \\ 0 \\ \beta_{x,y} + \beta_{y,x} \end{Bmatrix}, \quad \{\varepsilon_3\} = \begin{Bmatrix} \phi_{x,x} \\ \phi_{y,y} \\ 0 \\ \phi_{x,y} + \phi_{y,x} \end{Bmatrix} \tag{3c}$$

$$\{\gamma_0\} = \begin{Bmatrix} \theta_x + w_{0,x} \\ \theta_y + w_{0,y} \end{Bmatrix}, \quad \{\gamma_1\} = \begin{Bmatrix} 2\beta_x + w_{1,x} \\ 2\beta_y + w_{1,y} \end{Bmatrix}, \quad \{\gamma_2\} = \begin{Bmatrix} 3\phi_x + \Gamma_{,x} \\ 3\phi_y + \Gamma_{,y} \end{Bmatrix}. \tag{3d}$$

The subscript comma denotes the partial derivative with respect to the spatial coordinate succeeding it.

Based on the fiber-governed model, the constitutive relations for an arbitrary layer k in the laminate (x, y, z) coordinate system can be expressed as

$$\{\sigma\} = \{\, \sigma_{xx} \quad \sigma_{yy} \quad \sigma_{zz} \quad \tau_{xy} \quad \tau_{xz} \quad \tau_{yz} \,\}^{\mathrm{T}} = [\bar{Q}_{lk}] \begin{Bmatrix} \varepsilon_{\mathrm{bm}} \\ \varepsilon_s \end{Bmatrix}, \tag{4}$$

where the terms of constitutive matrix $[\bar{Q}_{lk}]$ of the kth ply are referred to the laminate axes. These can be obtained from the constitutive matrix $[Q_{lk}]$ relating the stress and strain components in the material principal directions (along the fiber and transverse directions) with the appropriate transformation as outlined in the literature [30]. The matrix $[Q_{lk}]$ can be expressed in terms of the Young's moduli, shear moduli and Poison's ratios of the material in tension or compression depending upon the sign of fiber direction strain. Here, the first subscript l refers to the bimodular characteristics: $l = 1$ denotes the properties associated with fiber-direction tension, $l = 2$ denotes those associated with fiber-direction compression. $\{\sigma\}$ and $\{\varepsilon\}$ are the stress and strain vectors, respectively. The superscript T refers the transpose of a matrix/vector.

The governing equations are obtained using Lagrange's equations of motion given by

$$\frac{\mathrm{d}}{\mathrm{d}t}[\partial(T - U)/\partial\dot{\delta}_i] - [\partial(T - U)/\partial\delta_i] = 0, \quad i = 1 \text{ to } n, \tag{5}$$

where T is the kinetic energy; U is the potential energy consisting of strain energy contributions due to the in-plane and transverse stresses. $\{\delta\} = \{\delta_1, \delta_2, ..., \delta_\iota, ..., \delta_n\}^{\mathrm{T}}$ is the vector of the degrees of freedom/generalized coordinates. A dot over the variable represents the partial derivative with respect to time. The kinetic energy of the plate is given by

$$T(\delta) = \frac{1}{2} \int \int \left[\sum_{k=1}^{n} \int_{h_k}^{h_{k+1}} \rho_k \{\dot{u}^k \;\; \dot{v}^k \;\; \dot{w}^k\} \{\dot{u}^k \;\; \dot{v}^k \;\; \dot{w}^k\}^{\mathrm{T}} \, \mathrm{d}z \right] \mathrm{d}x \, \mathrm{d}y, \tag{6}$$

where ρ_k is the mass density of the kth layer. h_k, h_{k+1} are the z-coordinates of the laminate corresponding to the bottom and top surfaces of the kth layer.

Using the kinematics given in Eq. (1), Eq. (6) can be rewritten as

$$T(\delta) = \frac{1}{2} \int \int \left[\sum_{k=1}^{n} \int_{h_k}^{h_{k+1}} \rho_k \{\dot{d}^e\}^{\mathrm{T}} [Z]^{\mathrm{T}} [Z] \{\dot{d}^e\} \, \mathrm{d}z \right] \mathrm{d}x \, \mathrm{d}y, \tag{7}$$

where $\{\dot{d}^e\}^{\mathrm{T}} = \{\dot{u}_0 \dot{v}_0 \dot{w}_0 \dot{\theta}_x \dot{\theta}_y \dot{w}_1 \dot{\beta}_x \dot{\beta}_y \dot{\Gamma} \dot{\phi}_x \dot{\phi}_y\}$ and

$$[Z] = \begin{bmatrix} 1 & 0 & 0 & z & 0 & 0 & z^2 & 0 & 0 & z^3 & 0 \\ 0 & 1 & 0 & 0 & z & 0 & 0 & z^2 & 0 & 0 & z^3 \\ 0 & 0 & 1 & 0 & 0 & z & 0 & 0 & z^2 & 0 & 0 \end{bmatrix}.$$

The potential energy functional U is given by

$$U(\delta) = \frac{1}{2} \int \int \left[\sum_{k=1}^{n} \int_{h_k}^{h_{K+1}} \{\sigma\}^{\mathrm{T}} \{\varepsilon\} \, \mathrm{d}z \right] \mathrm{d}x \, \mathrm{d}y. \tag{8}$$

Substituting the constitutive relation, Eq. (4), in Eq. (8), one can rewrite the potential energy functional U as

$$U(\delta) = \frac{1}{2} \int \int \left[\sum_{k=1}^{n} \int_{h_k}^{h_{k+1}} (\{\varepsilon_{\mathrm{bm}} \varepsilon_s\}^{\mathrm{T}} [\bar{Q}_{lk}] \{\varepsilon_{\mathrm{bm}} \varepsilon_s\}) \, \mathrm{d}z \right] \mathrm{d}x \, \mathrm{d}y. \tag{9}$$

For obtaining the element level governing equations, the kinetic and the total potential energies (T and U) may be conveniently rewritten as

$$T(\delta^e) = \frac{1}{2} \{\dot{\delta}^e\}^{\mathrm{T}} [M^e] \{\dot{\delta}^e\}, \tag{10}$$

$$U(\delta^e) = \frac{1}{2} \{\delta^e\}^{\mathrm{T}} [K^e] \{\delta^e\}. \tag{11}$$

Here, $[K^e]$ and $[M^e]$ are the elemental stiffness and mass matrices, and $\{\delta^e\}$ is the vector of the elemental degrees of freedom/generalized coordinates.

Substituting Eqs. (10) and (11) in Eq. (5), one obtains the governing equation for the element as

$$[M^e] \{\ddot{\delta}^e\} + [K^e] \{\delta^e\} = \{0\}. \tag{12}$$

The coefficients of mass and stiffness matrices involved in governing equation (12) can be rewritten as the product of the term having thickness coordinate z alone and the term containing x and y. In the present study, while performing the integration, terms having thickness coordinate z are explicitly integrated, whereas the terms containing x and y are evaluated using full integration with 3×3 points Gauss integration rule. Further while carrying out the integration along the z-direction, in addition to performing the integration in piecewise manner from layer to layer, the possibility of different properties (tension or compression) within a layer has also to be taken care.

Following the usual finite element assembly procedure, the governing equations of the laminate are obtained as

$$[M]\{\ddot{\delta}\} + [K]\{\delta\} = \{0\}, \tag{13}$$

where $[K]$ and $[M]$ are the global stiffness and mass matrices, respectively.

Eq. (13) can be solved using Newmark's direct time integration scheme for the free transient response analysis. The free vibration frequencies (ω) and associated mode shapes can be extracted from standard eigenvalue problem:

$$-\omega^2[M]\{\delta\} + [K]\{\delta\} = \{0\}. \tag{14}$$

3. Neutral surface location

The key element in the analysis of bimodular laminates is the determination of the neutral surface location. The portion of the laminate on one side of the neutral surface is in compression and the one on the other side is in tension. However, the location of the neutral surface is not known a priori. The location of the neutral surface is determined through the iterative solution.

If the neutral surface is located inside a layer (called the ''neutral surface layer'') instead of at the interface between two layers, the neutral surface layer is split into two layers. The neutral surface is determined using the zero fiber direction strain condition. An iteration procedure is necessary to determine the proper combination of the material properties and neutral surface. First, the neutral surface is assumed to be at the middle surface of the laminate for the purpose of initiating the iterative procedure. Then, any layer which straddles the neutral surface is split into two layers, a tension layer and a compression layer, and then the tension or compression properties are assigned to each layer. Based on this, the analysis is carried out and the deformation shape or normalized mode shape of interest is used for obtaining the new neutral surface location. This is repeated until the neutral surface location, frequencies and normalized mode shape from two consecutive iterations converge to a specified tolerance limit less than 0.001%. The above neutral surface iteration procedure is illustrated in Fig. 1. These steps are repeated for obtaining the frequencies corresponding to positive and negative half cycles of different modes.

4. Element description

In the present work, a C^0 continuous, eight-noded serendipity quadrilateral shear flexible plate element with 11 degrees of freedom (u_0, v_0, w_0, θ_x, θ_y , w_1, β_x, β_y , Γ, ϕ_x and ϕ_y: HSDT) developed based on the field consistency approach [31] is employed. The field variables are expressed in terms of their nodal values using shape functions as

$$(u_0, v_0, w_0, \theta_x, \theta_y, w_1, \beta_x, \beta_y, \Gamma, \phi_x, \phi_y) = \sum_{i=1}^{8} N_i^0(u_{0i}, v_{0i}, w_{0i}, \theta_{xi}, \theta_{yi}, w_{1i}, \beta_{xi}, \beta_{yi}, \Gamma_i, \phi_{xi}, \phi_{yi}), \tag{15}$$

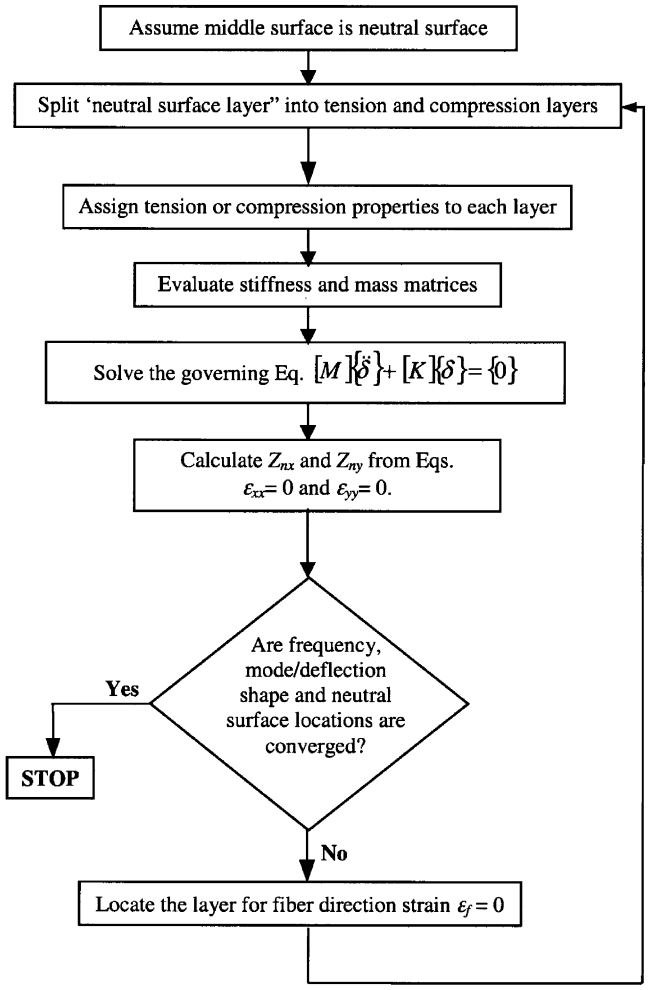

Fig. 1. Neutral surface iteration procedure.

where N_i^0 are the original shape functions for the eight-noded quadratic serendipity element. It can be noted here that the derivatives of shape functions $N_{i,x}^0$ and $N_{i,y}^0$ required for defining the various strain components within the element are linear in x and quadratic in y, and quadratic in x and linear in y, respectively, as the original interpolation functions are of quadratic type (in x and y) for the eight-noded element.

If the interpolation functions for an eight-noded element are used directly to interpolate the 11 field variables $u_o, \ldots, \phi_y$ in deriving the transverse shear strains, the element will lock and show oscillations in the transverse shear stresses. Field consistency requires that the transverse shear strains must be interpolated in a consistent manner [31]. This is achieved here by smoothing the original interpolation functions in a least-square fashion accurate to the desired form, i.e. the functions that are consistent with the derivative functions ($N_{i,x}^0$ or $N_{i,y}^0$). Here, the smoothed interpolation functions N_{xi}^1 and N_{yi}^1 consistent with derivative functions $w_{0,x}$ and

$w_{0,y}$ are required for the interpolation of θ_x and θ_y to be substituted in the expressions for the transverse shear strain components [$(\theta_x + w_{0,x})$ and $(\theta_y + w_{0,y})$] given in Eq. (3d), i.e. N^1_{xi} should be of the form linear in x and quadratic in y, and N^1_{yi} quadratic in x and linear in y, as outlined in Ref. [31].

Using the smoothed interpolation functions, the constrained transverse shear strain components are expressed as

$$(\theta_x + w_{0,x}) = \sum_{i=1}^{8} (N^1_{xi}\theta_{xi} + N^0_{i,x}w_{0i}), \tag{16a}$$

$$(\theta_y + w_{0,y}) = \sum_{i=1}^{8} (N^1_{yi}\theta_{yi} + N^0_{i,y}w_{0i}). \tag{16b}$$

The other strain fields are expressed in terms of original shape functions (N^0_i) and their derivatives.

The element thus derived is tested for static analysis of bimodular angle/cross-ply laminates subjected to thermal and mechanical loads, and is found free from the rank deficiency, shear locking and poor convergence syndrome [32,33].

5. Results and discussion

The study, here, is mainly concerned to predict the free flexural vibration characteristics of bimodulus laminated angle-ply plates employing field-consistent finite element developed based on higher-order theory. The first layer corresponds to the bottom-most layer and the ply angle is measured from x-axis in an anti-clockwise direction. All the layers are of equal thickness. Based on progressive mesh refinement, a 10×10 grid mesh is found to be adequate to model the full laminate for the present analysis.

The material properties considered in the present analysis in tension and compression are as follows [17,18]:

Material 1: $E_{1t} = 3.58\,\text{GPa}$, $E_{2t} = E_{3t} = 0.00909\,\text{GPa}$, $G_{12t} = G_{13t} = 0.0037\,\text{GPa}$, $G_{23t} = 0.0029\,\text{GPa}$, $v_{12t} = v_{23t} = v_{13t} = 0.416$.

$E_{1c} = E_{2c} = E_{3c} = 0.012\,\text{GPa}$, $G_{12c} = G_{13c} = 0.0037\,\text{GPa}$, $G_{23c} = 0.00499\,\text{GPa}$, $v_{12c} = v_{23c} = v_{13c} = 0.205$.

Here, the subscripts t and c refer to the tensile and compressive properties, respectively.

Material 2: $E_{1t} = 0.617\,\text{GPa}$, $E_{2t} = E_{3t} = 0.008\,\text{GPa}$, $G_{12t} = G_{13t} = 0.00262\,\text{GPa}$, $G_{23t} = 0.00233\,\text{GPa}$, $v_{12t} = v_{23t} = v_{13t} = 0.475$.

$E_{1c} = 0.0369\,\text{GPa}$, $E_{2c} = E_{3c} = 0.0106\,\text{GPa}$, $G_{12c} = G_{13c} = 0.00267\,\text{GPa}$, $G_{23c} = 0.00475\,\text{GPa}$, $v_{12c} = v_{23c} = v_{13c} = 0.185$.

Material 3: $E_{1t}/E_{2t} = 25$, $E_{2t} = E_{3t}$, $G_{12t}/E_{2t} = G_{13t}/E_{2t} = 0.5$, $G_{23t}/E_{2t} = 0.2$, $v_{12t} = v_{23t} = v_{13t} = 0.25$.

$E_{1c}/E_{2c} = 25$, $E_{2c} = E_{3c} = 1\,\text{GPa}$, $G_{12c}/E_{2c} = G_{13c}/E_{2c} = 0.5$, $G_{23c}/E_{2c} = 0.2$, $v_{12c} = v_{23c} = v_{13c} = 0.25$, $E_{2t}/E_{2c} = 0.2$.

The simply supported and clamped–clamped boundary conditions considered here are:
Simply supported:

$$v_0 = w_0 = \theta_y = w_1 = \Gamma = \beta_y = \phi_y = 0 \quad \text{at } x = 0, a,$$
$$u_0 = w_0 = \theta_x = w_1 = \Gamma = \beta_x = \phi_x = 0 \quad \text{at } y = 0, b.$$

Clamped–clamped:

$$u_0 = v_0 = w_0 = \theta_x = \theta_y = w_1 = \beta_x = \beta_y = \Gamma = \phi_x = \phi_y = 0 \quad \text{at } x = 0, a \text{ and } y = 0, b.$$

Here, a and b refer to the length and width of the plate, respectively.

The transverse displacement (w) and fiber direction strain (ε_f) presented here for free vibration time response analysis correspond to the (x, y) locations of $(a/2, b/2)$. Further, the non-dimensional forms used here for presentation of results are: frequencies (Ω_1, Ω_2) [$= (\omega_1, \omega_2)b^2(\rho/E_{2c}h^2)^{1/2}$; ω_1 and ω_2 are the frequencies in positive half and negative half cycles, respectively], average frequency $\Omega[= (1/2)(\Omega_1^{-1} + \Omega_2^{-1})^{-1}]$, transverse displacement $W[= w/h]$, neutral surface locations: $Z_{nx} = z_{nx}/h$ and $Z_{ny} = z_{ny}/h$, and time $\tau[= t/(4\pi^2 b^4 \rho/E_{2c}h^2)^{1/2}]$.

Before proceeding for the detailed study, the formulation developed herein is validated against available analytical solutions [27] for two-layered cross-ply simply supported rectangular bimodular laminates and the comparison of non-dimensional frequencies and neutral surface locations is highlighted in Table 1. It can be seen from this table that the present results are in good agreement with those in the literature [27]. It may be noted here that first-order shear deformation theory is employed in Ref. [27] and the results are presented for moderately thick rectangular plates ($b/h = 10$) for which the higher-order model results of present investigation are found to be close.

After the validation of the model, the time response analysis is carried out for two- and eight-layered cross/angle ply bimodular laminates to highlight the characteristic response behavior. The

Table 1
Comparison of nondimensional frequencies (Ω_1, Ω_2) and neutral surface locations (Z_{nx} and Z_{ny}) for different aspect ratios (a/b) of two-layered cross-ply ($0^\circ/90^\circ$) bimodular simply supported laminates ($b/h = 10$)

a/b	Ω_1		Ω_2		Z_{nx_1}		Z_{ny_1}		Z_{nx_2}		Z_{ny_2}	
	Present	Ref. [27]	Present	Ref. [27]	Present	Ref. [27]	Present	Ref. [27]	Present	Ref. [27]	Present	Ref. [27]
*Material*1												
0.5	13.8161	13.88	19.0495	19.38	−0.0164	−0.0171	0.4257	0.4247	0.4442	0.4457	−0.0639	−0.0648
0.7	9.3063	9.353	11.4760	11.60	−0.0235	−0.0240	0.4337	0.4338	0.4424	0.4434	−0.0480	−0.0490
1	6.9989	7.038	6.9989	7.038	−0.0343	−0.0347	0.4390	0.4394	0.4390	0.4394	−0.0343	−0.0347
1.4	6.0019	6.037	4.8264	4.838	−0.0487	−0.0494	0.4419	0.4423	0.4333	0.4335	−0.0245	−0.0250
2	5.5146	5.551	3.7112	3.712	−0.0700	−0.0705	0.4436	0.4437	0.4230	0.4228	−0.0172	−0.0174
*Material*2												
0.5	15.6341	15.95	18.2319	19.12	−0.0799	−0.0830	0.3598	0.3569	0.3632	0.3687	−0.1297	−0.1335
0.7	9.9024	10.04	11.1249	11.43	−0.0853	−0.0868	0.3606	0.3603	0.3634	0.3664	−0.1099	−0.1119
1	6.9963	7.085	6.9963	7.084	−0.0950	−0.0959	0.3622	0.3631	0.3622	0.3632	−0.0950	−0.0960
1.4	5.8459	5.928	5.1348	5.154	−0.1108	−0.1115	0.3635	0.3648	0.3593	0.3589	−0.0861	−0.0870
2	5.3551	5.435	4.2979	4.310	−0.1387	−0.1389	0.3645	0.3660	0.3532	0.3514	−0.0808	−0.0817

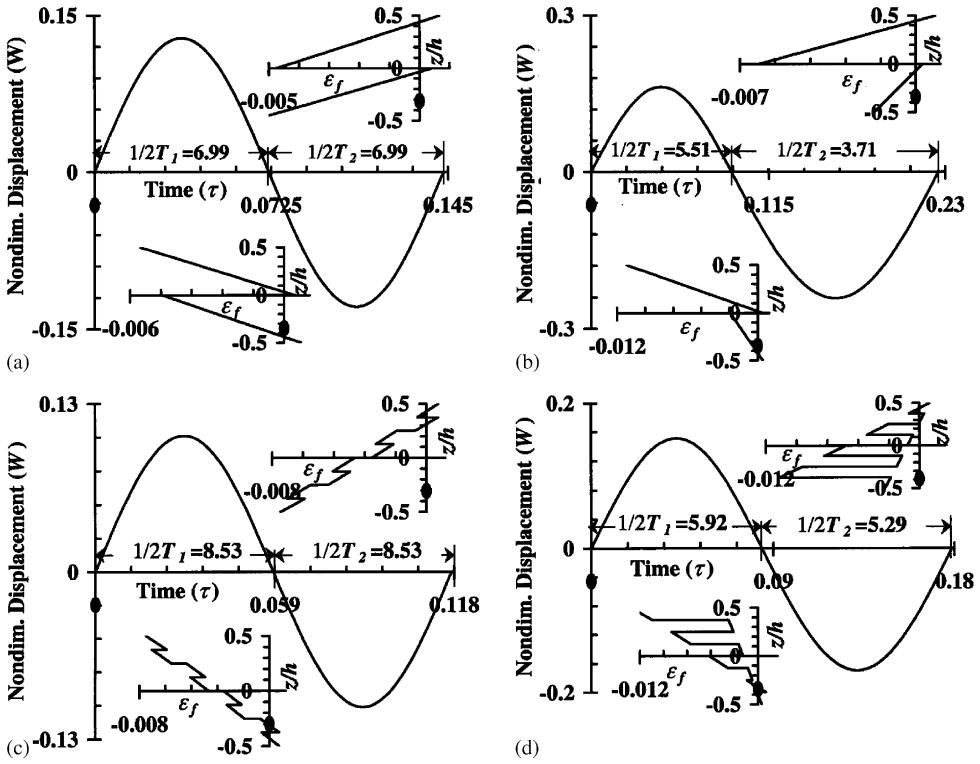

Fig. 2. Free vibration transient response of two- and eight-layered cross-ply simply supported laminates ($b/h = 10$): (a) two-layer ($0°/90°$), $a/b = 1$; (b) two-layer ($0°/90°$), $a/b = 2$; (c) eight-layer $(0°/90°)_4$, $a/b = 1$; (d) eight-layer $(0°/90°)_4$, $a/b = 2$.

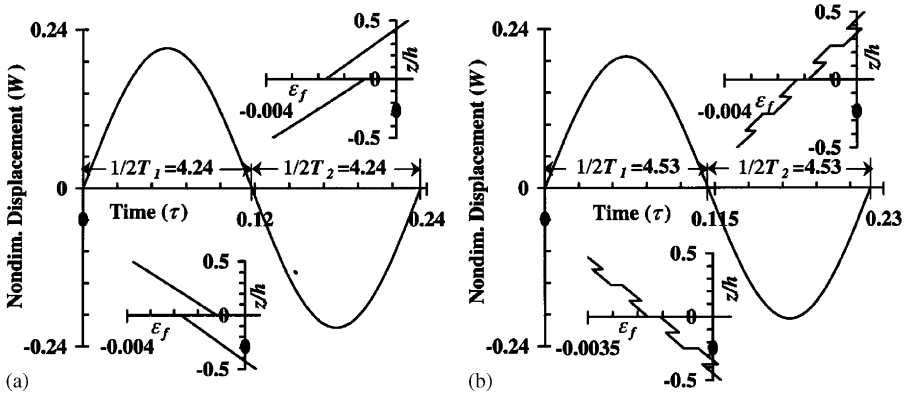

Fig. 3. Free vibration transient response of two- and eight-layered angle-ply simply supported laminates ($b/h = 10$): (a) two-layer ($15°/-15°$), $a/b = 2$; (b) eight-layer $(15°/-15°)_4$, $a/b = 2$.

initial conditions for the transient response analysis are assumed as zero displacement and non-zero velocity proportional to the fundamental mode shape obtained from eigenvalue analysis. The results are highlighted in Figs. 2 and 3 for cross-ply [$(0°/90°)$ and $(0°/90°)_4$] and angle-ply

$[(15^\circ/-15^\circ)$ and $(15^\circ/-15^\circ)_4]$ simply supported laminates ($b/h = 10$, $a/b = 1$, 2; Material 1). The inserted figures (in Figs. 2 and 3) depict the through the thickness fiber direction strain distribution during positive half cycle (upper inserted figure) and negative half cycle (lower inserted figure). These fiber direction strain distributions are important for the assignment of tensile/compressive properties to different layers. It can be observed from Fig. 2 that the time period and response amplitudes are different for positive and negative half cycles for cross-ply rectangular laminate cases ($a/b = 2$), whereas they are the same for square ($a/b = 1$) geometry. This information is not clearly brought out in the literature through transient free response analysis. However, for angle-ply laminates considered here, the time period and amplitude are the same, as depicted in Fig. 3, for positive and negative half cycles, irrespective of aspect ratio (a/b). It is apt to make a mention here that the response frequency values obtained from the response analysis match very well with those obtained from eigenvalue analysis. Therefore, detailed parametric studies are carried out using the eigenvalue approach.

The convergence of iterative eigenvalue approach for the determination of free vibration frequencies and mode shapes is highlighted in Figs. 4 and 5 for two-layered angle-ply ($\theta/-\theta$) simply supported square laminates ($b/h = 100, a/b = 1, \theta = 15^\circ, 45^\circ$). In these figures, the frequency values and corresponding mode shapes for the first three and last two consecutive iterations are presented. For the purpose of starting the iteration procedure, initially all the layers are assigned tensile properties. Then the analysis is carried out and the normalized mode shape of interest (with wavenumbers m along the x-axis and n along the y-axis) is used for evaluating the fiber direction strain distribution and, in turn, for property assignment. It may be emphasized here that for each mode combination $[(m,n) = (1,1),(1,2),(2,2)]$, the iteration procedure has to be carried out separately. It can be seen from these figures that the number of iterations required to achieve the converged results varies with the mode and geometrical/lamination parameters of the bimodular plate. It can also be viewed from these figures that, in general, the mode shapes (converged one) of bimodular plates are different from mode shapes of unimodular plates (results pertaining to the first iteration, wherein the tensile properties are used for the complete laminates). Further, the contour lines of the converged mode shapes show elongation along one diagonal and contraction along the other one for fundamental mode and higher mode with wavenumbers $(m,n) = (2,2)$.

Next, the influence of different geometrical and lamination scheme parameters of the plates on the fundamental frequencies is studied. The results are highlighted in Tables 2 and 3 for simply supported and clamped–clamped boundary conditions, respectively, considering different thickness ratios ($b/h = 5$, 10, 50 and 100), ply-angles ($\theta = 15^\circ$, $30^\circ$and 45°), number of layers ($N = 2,4,8$), and aspect ratios ($a/b = 1,2$). It can be observed from these tables that the frequency parameter, in general, increases with the increase in the number of layers, ply-angle and thickness ratio, whereas it shows decreasing trend with increase in a/b ratio. The variation of frequency parameter with number of layers or ply-angle is mostly linear for thick plate cases, whereas it varies nonlinearly for thin ones. The trend of frequency parameter change with thickness ratio (b/h) is nonlinear and the rate of increase of frequency parameter with respect to b/h is significantly more at lower b/h values compared to high b/h values for a chosen ply-angle and number of layers. The percentage change in the frequency parameter values with increasing number of layers is lowest for the 15°case and highest for the 45°case. Furthermore, the influence of ply-angle is more on frequency parameter values for thin square plate cases ($b/h = 100, 50$)

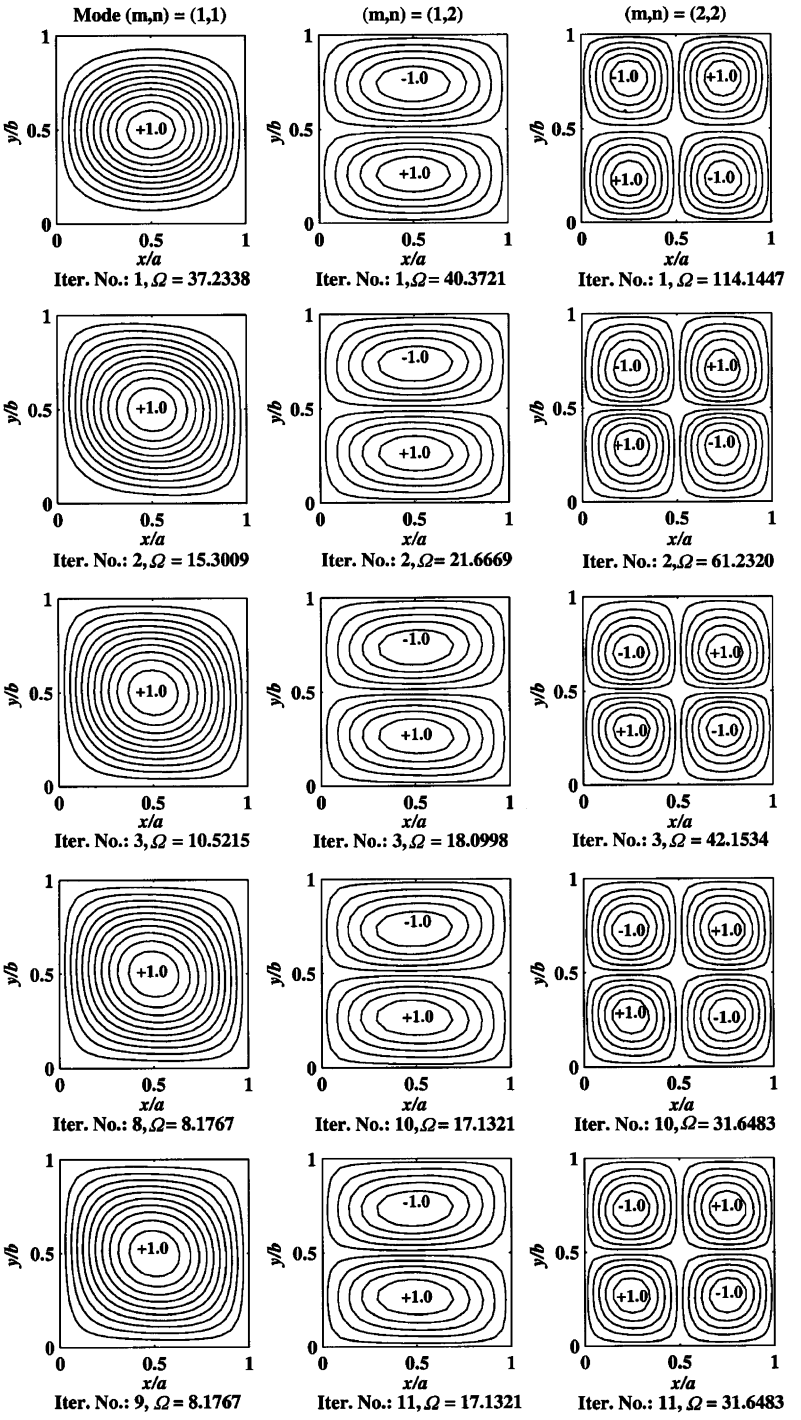

Fig. 4. Convergence study for frequency and mode shape of two-layered angle-ply square simply supported laminates $[(15^\circ/-15^\circ), b/h = 100, a/b = 1]$.

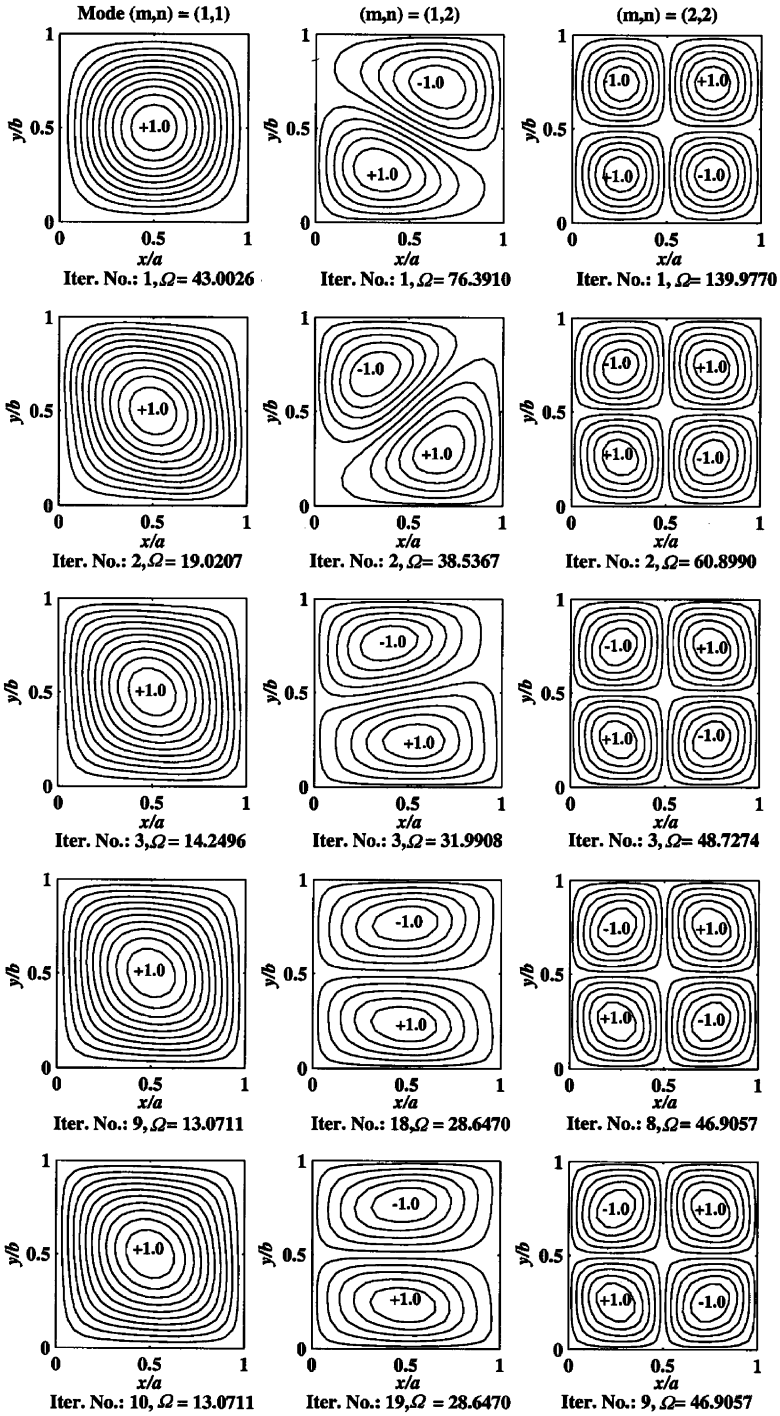

Fig. 5. Convergence study for frequency and mode shape of two-layered angle-ply square simply supported laminates $[(45^\circ/-45^\circ), b/h = 100, a/b = 1]$.

Table 2
Nondimensional fundamental frequencies (Ω) and neutral surface locations (Z_{nx} and Z_{ny}) for angle-ply $[(\theta/-\theta)_{N/2}]$ bimodular simply supported laminates ($a/b = 1, 2$; Material 1)

Thick. ratio (b/h)	Ply-angle (θ)	Number of layers (N)	Aspect ratio (a/b) = 1			$a/b = 2$		
			Ω	Z_{nx_1}	Z_{ny_1}	Ω	Z_{nx_1}	Z_{ny_1}
5	15	2	6.1241	−0.4229	0.1585	3.7759	0.4254	−0.0658
		4	6.2215	−0.4280	0.1752	3.8817	0.4832	−0.0854
		8	6.3809	−0.4554	0.1730	3.9775	0.5879	−0.0899
	30	2	6.8484	−0.4268	0.2123	4.7204	0.0564	0.0831
		4	7.1373	−0.5252	0.2711	5.1633	0.5685	0.1094
		8	7.4803	−0.6459	0.2991	5.4234	−0.1192	0.1218
	45	2	7.7202	−0.0869	−0.0869	4.9082	−0.1906	0.2619
		4	8.3996	−0.1936	−0.1936	5.2020	−0.1753	0.4142
		8	8.8751	−0.2715	−0.2715	5.5244	−0.1517	0.4947
10	15	2	7.2459	−0.4199	0.1660	4.2467	0.4313	−0.0692
		4	7.4103	−0.4240	0.1726	4.4169	0.5146	−0.0812
		8	7.6475	−0.4538	0.1477	4.5317	0.6278	−0.0800
	30	2	8.4597	−0.4421	0.2091	5.7781	−0.0641	0.1308
		4	8.9652	−0.5700	0.2407	6.6405	0.0044	0.2341
		8	9.5011	−0.6954	0.2457	7.0348	0.0982	0.2462
	45	2	10.2474	−0.0718	−0.0718	5.7914	−0.1941	0.2809
		4	11.7086	−0.1821	−0.1821	6.2413	−0.1438	0.4437
		8	12.4408	−0.2332	−0.2332	6.7171	−0.1047	0.5281
50	15	2	8.0668	−0.4173	0.1700	4.7019	0.4297	−0.0744
		4	8.2907	−0.4211	0.1656	4.9288	0.5365	−0.0829
		8	8.5917	−0.4549	0.1291	5.0649	0.6514	−0.0793
	30	2	9.6532	−0.4555	0.2141	6.6568	−0.1629	0.1553
		4	10.3746	−0.6145	0.2309	8.1713	−0.2985	0.3955
		8	11.1093	−0.7457	0.2295	8.8300	−0.3468	0.4435
	45	2	12.8303	−0.0488	−0.0488	6.3213	−0.2138	0.2888
		4	16.2946	−0.1466	−0.1466	6.8989	−0.1428	0.4599
		8	17.6408	−0.1841	−0.1841	7.4954	−0.1008	0.5515
100	15	2	8.1767	−0.4170	0.1689	4.7768	0.4267	−0.0750
		4	8.4022	−0.4212	0.1645	5.0079	0.5362	−0.0844
		8	8.7089	−0.4559	0.1289	5.1442	0.6491	−0.0814
	30	2	9.7596	−0.4555	0.2157	6.7428	−0.1787	0.1569
		4	10.5059	−0.6177	0.2343	8.3406	−0.3366	0.4018
		8	11.2598	−0.7486	0.2321	9.0507	−0.4109	0.4528
	45	2	13.0711	−0.0428	−0.0428	6.3634	−0.2204	0.2894
		4	16.8474	−0.1387	−0.1387	6.9534	−0.1510	0.4615
		8	18.3532	−0.1697	−0.1697	7.5569	−0.1106	0.5549

compared to thick and moderately thick ones ($b/h = 5, 10$). It is also revealed from these tables that the neutral surface locations, in general, shift towards outer surfaces with increase in the number of layers. The influence of lamination parameters on the fundamental frequencies of rectangular plates is less compared to square ones. It can also be inferred from Tables 2 and 3 that

Table 3
Nondimensional fundamental frequencies (Ω) and neutral surface locations (Z_{nx} and Z_{ny}) for angle-ply $[(\theta/-\theta)_{N/2}]$ bimodular clamped–clamped laminates ($a/b = 1, 2$; Material 1)

Thick. ratio (b/h)	Ply-angle (θ)	Number of layers (N)	Aspect ratio (a/b) = 1			$a/b = 2$		
			Ω	Z_{nx_1}	Z_{ny_1}	Ω	Z_{nx_1}	Z_{ny_1}
5	15	2	9.7810	−0.1937	−0.0075	6.4128	−0.0781	0.0004
		4	10.0595	−0.0092	0.0278	6.6739	−0.3765	0.0266
		8	10.4685	−0.0319	0.0343	6.9648	−0.0072	0.0482
	30	2	9.8881	−0.1278	−0.0061	7.0014	−0.0924	−0.0187
		4	10.5133	−0.0210	0.0378	7.7009	−0.4227	−0.0020
		8	11.1173	−0.0361	0.0169	8.2725	−0.5413	0.0716
	45	2	9.9805	−0.0472	−0.0472	7.6248	−0.0288	−0.0573
		4	10.6922	0.0884	0.0885	8.2844	−0.0450	0.1043
		8	11.3291	−0.0456	−0.0457	8.7853	−0.3002	−0.1196
10	15	2	16.8911	−0.0148	−0.0227	9.2340	−0.0191	−0.0149
		4	17.7160	−0.2984	0.0096	10.2351	−0.2552	0.0035
		8	18.4634	−0.0288	0.0415	10.7150	−0.3291	0.0147
	30	2	17.0586	−0.0487	−0.0490	10.7934	−0.1015	−0.0199
		4	18.9282	−0.3280	0.0119	12.9490	−0.3679	−0.0346
		8	20.1098	0.0468	0.0563	13.9483	−0.6631	−0.0064
	45	2	17.1940	−0.0572	−0.0572	12.7948	−0.0960	−0.0361
		4	19.5727	−0.1325	−0.1326	14.8335	−0.0785	−0.1425
		8	20.9926	−0.0998	−0.0995	15.9626	−0.0449	−0.1058
50	15	2	35.4195	−0.0334	−0.1057	13.2195	−0.0305	−0.0478
		4	48.8876	−0.1202	−0.2038	18.2098	−0.1341	−0.1268
		8	52.5226	−0.0922	−0.2144	19.7126	−0.1299	−0.1365
	30	2	33.5983	−0.0332	−0.1197	16.4397	−0.1005	−0.0290
		4	49.8249	−0.1227	−0.2057	24.9614	−0.2426	−0.0770
		8	54.2786	−0.1090	−0.2037	27.3692	−0.2706	−0.0783
	45	2	33.5368	−0.0670	−0.0670	21.7393	−0.1406	−0.0368
		4	50.4590	−0.1562	−0.1562	33.4867	−0.2630	−0.1084
		8	55.1834	−0.1655	−0.1655	36.8801	−0.3010	−0.0868
100	15	2	38.1568	−0.0375	−0.1195	13.6794	−0.0309	−0.0526
		4	56.8667	−0.1160	−0.2720	19.3394	−0.1236	−0.1405
		8	62.4386	−0.0924	−0.3176	21.0480	−0.1220	−0.1572
	30	2	35.9713	−0.0356	−0.1217	17.0925	−0.1007	−0.0294
		4	56.9481	−0.1172	−0.2346	26.8356	−0.2324	−0.0784
		8	62.9164	−0.1081	−0.2623	29.5547	−0.2563	−0.0847
	45	2	35.9629	−0.0678	−0.0678	22.7849	−0.1421	−0.0361
		4	57.5299	−0.1579	−0.1579	36.6490	−0.2733	−0.1037
		8	63.5545	−0.1770	−0.1770	40.6301	−0.3132	−0.0914

the behavior of clamped–clamped plates is qualitatively similar to that of simply supported ones. However, the frequency values are significantly higher and their variation with different geometrical/lamination parameters is more for clamped–clamped plates compared to simply supported cases.

A detailed study is also carried out to highlight the variation of higher-mode frequencies with geometrical and lamination scheme parameters and the results are presented in Table 4. In general, the behavior is qualitatively similar to that corresponding to the fundamental mode. However, the effect of number of layers is more in optimizing the frequency values corresponding

Table 4
Nondimensional higher mode frequencies (Ω) for angle-ply $[(\theta/-\theta)_{N/2}]$ bimodular simply supported laminates ($a/b = 1, 2$; Material 1)

Thick. ratio (b/h)	Ply-angle (θ)	Number of layers (N)	Aspect ratio (a/b) = 1			$a/b = 2$		
			$(m,n) = (1,2)$	(2, 1)	(2,2)	$(m,n) = (1,2)$	(2, 1)	(2,2)
5	15	2	11.4499	10.5923	13.8353	9.9630	5.8760	11.1751
		4	11.6224	11.2508	13.8409	9.9686	6.6621	11.3080
		8	11.8115	11.3637	13.8421	10.0134	7.1167	11.4155
	30	2	12.0896	11.8859	12.6085	10.9540	7.2803	12.3076
		4	12.2890	12.3745	13.3078	11.9547	8.1595	12.5941
		8	12.4698	12.5750	13.8588	12.6455	8.7861	12.8127
	45	2	13.6201	13.6201	19.9291	10.7857	6.8646	13.1890
		4	14.9223	14.9223	20.2513	11.7245	7.6079	13.4608
		8	15.8196	15.8196	21.5670	12.3381	8.1971	13.8595
10	15	2	14.4132	17.3426	24.0690	11.9302	7.7885	14.5097
		4	14.6483	17.9364	24.2124	12.0366	8.7380	15.3453
		8	14.9857	18.5295	24.2185	12.1606	9.3634	16.9661
	30	2	16.3290	17.6520	24.2486	14.3524	9.7007	17.5698
		4	17.1297	19.0760	24.7231	16.4057	11.4842	20.0023
		8	17.9143	20.1250	25.1203	17.9120	12.5352	21.8124
	45	2	19.5423	19.5423	28.3080	14.6266	8.7290	18.0518
		4	22.6867	22.6867	34.2368	16.1266	9.9124	19.0249
		8	24.6390	24.6390	36.1461	17.1964	10.8649	20.5715
50	15	2	16.8074	22.8794	33.9567	13.5685	9.1547	17.2495
		4	17.2565	23.7267	34.5051	13.8801	10.5309	19.1525
		8	17.7657	24.5370	34.9138	14.1126	11.3674	20.9610
	30	2	20.2455	23.1988	33.9276	17.7566	12.1080	27.2160
		4	22.2483	26.2962	43.0186	21.9551	15.7994	31.4080
		8	23.9132	28.6667	43.9351	24.1802	17.5839	35.4384
	45	2	27.6581	27.6581	44.2413	17.7835	10.1062	23.3026
		4	36.1460	36.1460	60.1528	20.3178	11.8178	26.6586
		8	40.0933	40.0933	68.6894	22.2548	13.1671	29.5616
100	15	2	17.1321	23.3195	31.6483	13.7937	9.3253	17.7135
		4	17.5960	24.2044	33.9569	14.1328	10.7461	19.7198
		8	18.1136	25.0395	35.9233	14.3807	11.5987	21.5876
	30	2	20.6617	23.6753	34.9534	18.1356	12.4054	28.0739
		4	22.8080	26.9440	41.0757	22.6133	16.3691	33.2917
		8	24.5831	29.4277	45.9600	24.9316	18.2645	37.6153
	45	2	28.6470	28.6470	46.9057	18.0539	10.2579	23.8701
		4	38.2944	38.2944	66.4517	20.6517	12.0184	27.8030
		8	42.6016	42.6016	78.8389	22.6493	13.3994	30.4875

Table 5
Nondimensional fundamental frequencies (Ω) and neutral surface locations (Z_{nx} and Z_{ny}) for angle-ply $[(\theta/-\theta)_{N/2}]$ square simply supported laminates ($a/b = 1$; Material 3)

Thick. ratio (b/h)	Ply-angle (θ)	Number of layers (N)	Ω	Z_{nx_1}	Z_{ny_1}	Z_{nx_2}	Z_{ny_2}
5	15	2	6.3304	−0.1732	−0.0455	0.1738	0.0455
		4	6.2747	0.0657	−0.0525	−0.0655	0.0529
		8	6.5815	0.0795	−0.0067	−0.0795	0.0066
	30	2	6.5201	−0.1365	0.0107	0.1371	−0.0109
		4	6.4114	0.1390	0.1047	−0.1502	−0.1072
		8	6.7897	0.1199	0.2130	−0.1557	−0.2133
	45	2	6.7132	−0.0280	−0.0280	0.0284	0.0284
		4	6.6582	−0.1814	−0.1814	0.1814	0.1814
		8	6.9754	0.0463	0.0463	−0.0461	−0.0461
100	15	2	9.0667	0.1356	0.1024	−0.1352	−0.1019
		4	10.1666	0.1855	0.1855	−0.1853	−0.0691
		8	10.5366	0.2015	0.0707	−0.2014	−0.0706
	30	2	9.6456	0.1557	−0.0222	−0.1547	0.0225
		4	11.7408	0.2544	−0.0796	−0.2538	0.0795
		8	12.3499	0.2845	−0.0997	−0.2842	0.0996
	45	2	10.4243	0.0490	0.0490	−0.0490	−0.0490
		4	12.8296	0.0960	0.0960	−0.0961	−0.0961
		8	13.4518	0.1014	0.1014	−0.1015	−0.1015

to modes with $(m, n) = (2, 1)$ and (2,2) for rectangular laminates compared to square ones. Further, it can be noticed from Table 3 that the frequency parameter values corresponding to mode (1, 2) are lower compared to those of (2, 1) mode for square laminates with ply-angles 15°and 30°, whereas they are the same for the 45°case as expected. But, the combined influence of ply-angle and aspect ratio for rectangular case leads to significantly lower frequency parameter values for the (2, 1) mode compared to those of the (1, 2) mode.

Finally, the fundamental frequency parameters for bimodular thick and thin plates with compressive properties higher than the tensile ones (Material 3) are depicted in Table 5. It can be revealed from this table that the variation of frequency parameter with ply-angle is mostly linear even for thin plates unlike the plates of Material 1, and in addition, four-layered thick laminates yield lower frequency values compared to those of two-layered thick plates. Further, the frequency parameter values are higher for the 15°ply-angle case and lower for the 45°ply-angle case compared to those of Material 1 (see Table 2), whereas for 30°cases it depends on the thickness ratio and number of layers. The location of neutral surfaces is significantly closer to the middle surface compared to Material 1 cases.

6. Conclusions

The free flexural vibration analysis of bimodular angle-ply laminated composite plates is carried out using field-consistent finite element based on higher order theory incorporating cross-sectional

warping and transverse normal deformation through nonlinear approximation of in-plane and transverse displacement components. The parametric studies are made to provide some insight into the effects of plate geometry, lay-up, ply-angle, the material properties and boundary conditions on the free flexural vibration response and frequencies, neutral surface locations and mode shapes of bimodulus angle-ply composite laminates. From the detailed parametric study, the following conclusions can be drawn:

(i) Time period and response amplitudes are different for positive and negative half cycles of vibrations for cross-ply rectangular laminates, whereas they are the same for cross-ply square and angle-ply plates.
(ii) Mode shapes of bimodular plates are different from those of unimodular plates and their contour lines show elongation along one diagonal and contraction along the other one.
(iii) The frequency parameter, in general, increases with the increase in the number of layers, ply-angle and thickness ratio, whereas it shows decreasing trend with increase in aspect ratio.
(iv) The variation of frequency parameter with the number of layers or ply-angle is mostly linear for thick plate cases, whereas it varies nonlinearly for thin ones.
(v) The percentage change in the frequency parameter values with increasing number of layers is the lowest for the 15°case and highest for the 45°case.
(vi) Effect of lamination scheme is more on frequency parameter values for thin plates compared to thick and moderately thick ones, particularly, more so for square plates.
(vii) The frequency values are significantly higher and their variation with different geometrical/lamination parameters is more for clamped–clamped plates compared to simply supported ones.
(viii) Neutral surface locations, in general, shift towards outer surfaces with increase in the number of layers.
(ix) Frequency parameter values corresponding to mode (1, 2) are lower compared to those of (2, 1) mode for square laminates with 15°and 30°ply-angles, whereas the combined influence of ply-angle and aspect ratio for rectangular plates leads to significantly lower frequency parameter values for the (2, 1) mode compared to those of (1, 2) mode.
(x) Neutral surface locations are significantly closer to the middle surface for plates of Material 3 compared to those of Material 1.

References

[1] C.W. Bert, Models for fibrous composites with different properties in tension and compression, *Journal of Engineering Materials and Technology, Transactions of the ASME* 99H (1977) 344–349.
[2] R.M. Jones, H.S. Morgan, Bending and extension of cross-ply laminates with different moduli in tension and compression, *Computers and Structures* 11 (1980) 181–190.
[3] C.W. Bert, J.N. Reddy, Mechanics of bimodular composite structures, in: Z. Hashin, C.T. Herakovich (Eds.), *Mechanics of Composite Materials: Recent Advances, Proceedings of the IUTAM Symposium*, Virginia Polytech. Inst., Blacksburg, VA, Pergamon, Oxford, 1983, pp. 323–364.
[4] J.N. Reddy, W.C. Chao, Finite element analysis of laminated bimodulus composite-material plates, *Computers and Structures* 12 (1980) 245–251.

[5] J.N. Reddy, C.W. Bert, On the behavior of plates laminated of bimodulus composite materials, *ZAMM* 62 (1982) 213–219.
[6] S.V. Hoa, J. Maji, Two-dimensional bending and extension of cross-ply laminates with different moduli in tension and compression, *Computers and Structures* 20 (1985) 921–928.
[7] J.N. Reddy, C.W. Bert, Behavior of plates laminated of bimodulus composite materials, in: K. Kawata, T. Akasaka (Eds.), *Composite Materials*, Proceedings of the Japan–US Conference, Tokyo, vol. 8, 1981, pp. 89–101.
[8] J.N. Reddy, W.C. Chao, Nonlinear bending of bimodular-material plates, *International Journal of Solids and Structures* 19 (1983) 229–237.
[9] C.W. Bert, V.S. Reddy, S.K. Kincannon, Deflection of thin rectangular plates of cross-plied bimodulus material, *Journal of Structural Mechanics* 8 (1980) 347–364.
[10] C.W. Bert, J.N. Reddy, V.S. Reddy, W.C. Chao, Bending of thick rectangular plates laminated of bimodulus materials, *AIAA Journal* 19 (1981) 1342–1349.
[11] S.K. Kincannon, C.W. Bert, V.S. Reddy, Cross-ply elliptic plates of bimodulus materials, *Journal of Structural Division, Proceedings of the ASCE* 106 (1980) 1437–1449.
[12] J.N. Reddy, C.W. Bert, Y.S. Hsu, V.S. Reddy, Thermal bending of thick rectangular plates of bimodulus composite materials, *Journal of Mechanical Engineering Science* 22 (1980) 297–304.
[13] F. Gordaninejad, A finite element model for the analysis of thick, anisotropic, bimodular, fibrous-composite plates, *Computers and Structures* 31 (1989) 907–912.
[14] F. Gordaninejad, Nonlinear bending of anisotropic bimodular composite-material plates, *Computers and Structures* 33 (1989) 615–620.
[15] N.J. Pagano, Exact solutions for rectangular bidirectional composites and sandwich plates, *Journal of Composite Materials* 4 (1970) 20–34.
[16] K. Bhaskar, T.K. Varadan, J.S.M. Ali, Thermoelastic solutions for orthotropic and anisotropic composite laminates, *Composites Part B: Engineering* 27 (1996) 415–420.
[17] Y.P. Tseng, C.T. Lee, Bending analysis of bimodular laminates using a higher-order finite strip method, *Composite Structures* 30 (1995) 341–350.
[18] C.P. Fung, J.L. Doong, Bending of a bimodulus laminated plate based on a higher-order shear deformation theory, *Composite Structures* 10 (1988) 121–144.
[19] T. Iwase, K.I. Hirashima, High-accuracy analysis of beams of bimodulus materials, *Journal of Engineering Mechanics* 2 (2000) 149–156.
[20] Y.P. Tseng, Y.C. Jiang, Stress analysis of bimodulus laminates using hybrid stress plate elements, *International Journal of Solids and Structures* 35 (1988) 2025–2038.
[21] R. Zinno, F. Greco, Damage evolution in bimodular laminated composites under cyclic loading, *Composite Structures* 53 (2001) 381–402.
[22] J.L. Doong, L.W. Chen, Axisymmetric vibration of an initially stressed bimodulus thick circular plate, *Journal of Sound and Vibration* 94 (1984) 461–468.
[23] L.W. Chen, D.P. Juang, Axisymmetric vibration of bimodulus thick circular and annular plates, *Computers and Structures* 25 (1987) 759–764.
[24] L.-W. Chen, C.C. Chen, Asymmetric vibration and dynamic stability of bimodulus thick annular plates, *Computers and Structures* 31 (1989) 1013–1022.
[25] C.W. Bert, A.D. Tran, Transient response of a thick beam of bimodular material, *Earthquake Engineering and Structural Dynamics* 10 (1982) 551–560.
[26] J.N. Reddy, Transient response of laminated, bimodular-material, composite rectangular plates, *Journal of Composite Materials* 16 (1982) 139–152.
[27] C.W. Bert, J.N. Reddy, W.C. Chao, V.S. Reddy, Vibration of thick rectangular plates of bimodulus composite material, *ASME Journal of Applied Mechanics* 48 (1981) 371–376.
[28] J.L. Doong, L.W. Chen, Vibration of a bimodulus thick plate, *ASME Journal of Vibration, Acoustics, Stress and Reliability Design* 107 (1985) 92–97.
[29] C.W. Bert, M. Kumar, Vibration of cylindrical shells of bimodulus composite materials, *Journal of Sound and Vibration* 81 (1982) 107–121.
[30] R.M. Jones, *Mechanics of Composite Materials*, McGraw-Hill, New York, 1975.

[31] G. Prathap, B.P. Naganarayana, B.R. Somashekar, Field-consistency analysis of the isoparametric eight-noded plate bending element, *Computers and Structures* 29 (1988) 857–873.
[32] B.P. Patel, A.V. Lele, M. Ganapathi, S.S. Gupta, C.T. Sambandam, Thermo-flexural analysis of thick laminates of bimodulus composite materials, *Composite Structures* 63 (2004) 11–20.
[33] M. Ganapathi, B.P. Patel, A.V. Lele, Static analysis of bimodulus laminated composite plates subjected to mechanical loads using higher-order shear deformation theory, *Journal of Reinforced Plastics and Composites* 23 (2004) 1159–1171.